

An experimental study on the role of compliant elements on the locomotion of the self-reconfigurable modular robots Roombots

Massimo Vespignani*, Emmanuel Senft, Stéphane Bonardi, Rico Moeckel, and Auke J. Ijspeert

Abstract—This paper presents the results of a study on the exploitation of compliance in structures made of self-reconfigurable modular robots - Roombots. This research was driven by the following three hypotheses: (1) compliance can improve locomotion performance; (2) different types of compliance will result in diverse locomotion behaviors; (3) control parameters optimized for a medium level of compliance will perform better for other values of compliance than parameters optimized for extremal compliance. Two types of in-series compliant elements were tested, with five different stiffness values for each of them, on a structure made of two Roombots modules. We ran dedicated on-line locomotion parameter optimizations for six different configurations and evaluated their performance for different stiffness values. Hypothesis 1 was confirmed for both types of compliant elements, with a peak of performance for an optimal level of compliance. The variety of locomotion strategies obtained for the different structures confirms hypothesis 2. Hypothesis 3 was only partially confirmed.

I. INTRODUCTION

Self-reconfigurable modular robots (SRMR) are cellular robots capable of adapting their shape and functions to new environmental conditions by rearranging the connectivity of their basic elements (modules) [1]. Each module is an autonomous robot with a fairly limited number of features and equipped with one or more connection ports that allow it to connect to the neighboring elements. One of the challenges in the field of SRMR is to design modules strong enough to be able to lift several times their own weight. For this reason, many robots in literature are designed with large torque capability (e.g. with high reduction ratio gearboxes), resulting in rather slow speeds and non-dynamic gaits [2].

This research study aims at investigating whether compliance can be beneficial for the locomotion of self-reconfigurable modular robots, pushing their physical performance boundaries (e.g. getting more dynamical and energy efficient gaits by storing and releasing elastic energy) and reducing the complexity of their control system (e.g. to passively adapt to the shape of the terrain [3]), with the ultimate goal of contributing to the hardware scalability challenge [4]. To pursue this objective, we are investigating the effect on flat-ground locomotion of added in-series compliance in the inter-connection between two SRMR, using Roombots (RB) [5] as robotic tool (Figs. 1 and 2).

* The authors are with the Institute of Bioengineering, École Polytechnique Fédérale de Lausanne (EPFL), 1015 - Lausanne, Switzerland. Corresponding author: Massimo Vespignani, massimo.vespignani@epfl.ch

This work was supported by the Swiss National Science Foundation through the National Centre of Competence in Research (NCCR) Robotics and by the European Community's Seventh Framework Programme FP7/2007-2013 - Future Emerging Technologies, Embodied Intelligence, under the grant agreement no. 231688 (Locomorph).

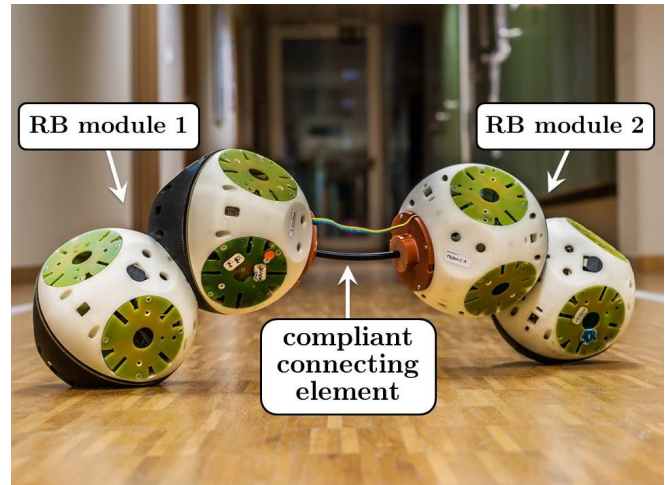


Fig. 1: Two Roombots (RB) modules interconnected with a compliant rod.

The current work is guided by the following three main hypotheses:

- 1) Compliance can improve the locomotion performances of a SRMR. Among the several factors that can define the performance of locomotion, we considered the speed (displacement divided by elapsed time) of the gait and its repeatability.
- 2) Different types of compliant elements will produce a significantly different behavior. As a first exploration, for this study we analyzed the effect of a torsional and of an omnidirectional spring.
- 3) When testing a set of compliant elements with different values of stiffness, the locomotion control parameters optimized for an intermediate value of the set will perform better when tested on any other member than the control parameters optimized for the stiffest or the softest element in the set.

A. Related Work

While the role of compliance in a monolithic robotic structure has long been suggested and studied, for instance in the field of articulated locomotion [6][7], to the best of our knowledge this is still a scarcely explored topic in the field of reconfigurable modular robotics.

Previous work has been done by Aoi et al. [8], who investigated the role of joint compliance in achieving high maneuverability for the locomotion of a simulated multi-legged modular robot. Yu et al. [9] presented Morpho, a

self-deformable modular robot where active and passive links work together to shape the structure into different geometries.

The work that reflects more closely our objectives of exploring and exploiting the effect of compliance in a (self) reconfigurable modular robot was done by Sastra et al. [10][11]. In their research, they used their reconfigurable modular robot CKBot as a tool to quickly build robotic structures with different morphologies and explore a novel biologically-inspired legged style of locomotion. They designed a set of purely passive compliant legs for CKBot in order to increase its dynamics and show a bouncing gait that runs like a Lateral Leg Spring (LLS) model.

Our approach differs from the state of the art because we are exploring elements that can be kept during self-reconfiguration (as opposed to elements that need to be removed/clipped), passive elements to which the robot can connect when it needs to change the stiffness/compliance of some of its parts to adapt to new conditions (although this feature is not tested here). In this regard, we are also exploring how to tackle the problem of controlling such a self-reconfigurable modular robot, with a focus on how to minimize the number of locomotion parameter optimizations needed to have efficient gaits after a change in structural compliance.

II. MATERIALS AND METHODS

A. Roombots

In order to study the effect of multiple types of compliance in several structures, we used the self-reconfigurable modular robots Roombots (RB) [12]. Each RB module is a fully autonomous robot made of four hemispheres, with three continuous rotational degrees of freedom and 10 genderless (active or passive) four-way symmetric connection ports (Fig. 2; detailed specifications are summarized in Table I).

Roombots are an efficient rapid prototyping tool to study locomotion control of articulated robots. Their mechanical connection mechanisms allow to quickly assemble new structures and investigate the effect of morphology in the



(a) RB module

(b) RB actuators

Fig. 2: (a) Roombots (RB) module with a passive (top) and an active (bottom) four-way symmetric genderless connection port. (b) Placement and orientation of the RB actuators: one inner (gray) and two outer (red) continuous rotational degrees of freedom.

resulting gait. Given the 4-way symmetry and the large number of available connection ports per module, the number of possible configurations can be quite large (limited by the maximum achievable motor torque), resulting in a large variety of structures that can be explored, each with completely different behaviors and workspace.

In the current work, we used two RB modules interconnected in PER configuration¹, with the compliant elements mounted in-series between them. To simplify the intercommunication between the modules, we used a wired communication channel.

B. Compliant elements

For the experiments described in this paper, we analyzed the effect of added compliance in the interconnection between modules. We focused on two different types of compliance, namely omnidirectional and torsional compliance, and we manufactured a set of five compliant elements with different stiffness values for each of these two categories (Fig. 3 and Table II).

The basic element of the first set, referred as compliant rod (CR), is a cylindrical beam made of polyoxymethylene (POM), blocked on each side (Fig. 3a). By changing the diameter of the beam, we were able to produce different stiffness values. The length of the beam is fixed at 0.081m so that the total length of the element (including the fixation on each side) is equal to the basic Roombots grid size (0.11m). Given the axial symmetry, the CR can bend in every direction perpendicular to its longer axis. The CR elements have also some torsional stiffness (torsion of a beam), but its effect was considered minimal when compared with the bending of the beam or to the elements used to study the torsional compliance.

To recreate pure torsional compliance, we developed two different designs of torsional springs (TS). The first design

TABLE I: Hardware specifications of a Roombots module.

Specification	Value
Degrees of freedom	3 (continuous rotational)
Outer motors	Faulhaber 2342 012 CR
Inner motor	Faulhaber 2232 012 SR
Outer gearboxes reduction	305:1
Inner gearbox reduction	366:1
Outer dofs speed (No load)	26.6 RPM
Inner dof speed (No load)	19.4 RPM
Outer dofs nominal torque	4.9 Nm
Inner dof nominal torque	3.6 Nm
Number of connection ports	10 (active or passive)
Active connection type	4-way symmetric genderless mechanical latches
Overall dimensions	110x 110x 220 mm
Weight	1.4 kg
Communication	Bluetooth
Energy source	4-cell LiPo battery, 1200 mAh autonomy \sim 1 hour

¹For a description of the Roombots naming convention, see [5]

TABLE II: Compliant elements specifications. k_{C_x} : cantilever beam stiffness (from eq. 1); k_{T_x} : beam’s torsional stiffness (from eq. 2); k_x : torsional spring stiffness (from datasheet (TS1–TS4)) or FEA (TS5)).

Item name	Stiffness value
Compliant Rod 1 (5 mm)	k_{C_1} $537Nm^{-1}$
	k_{T_2} $66Nmm\ deg^{-1}$
Compliant Rod 2 (6 mm)	k_{C_2} $1113Nm^{-1}$
	k_{T_2} $137Nmm\ deg^{-1}$
Compliant Rod 3 (7 mm)	k_{C_3} $2062Nm^{-1}$
	k_{T_3} $254Nmm\ deg^{-1}$
Compliant Rod 4 (8 mm)	k_{C_4} $3518Nm^{-1}$
	k_{T_4} $433Nmm\ deg^{-1}$
Compliant Rod 5 (12 mm)	k_{C_5} $17811Nm^{-1}$
	k_{T_5} $2193Nmm\ deg^{-1}$
Torsional Spring 1	k_1 $7.76Nmm\ deg^{-1}$
Torsional Spring 2	k_2 $10.16Nmm\ deg^{-1}$
Torsional Spring 3	k_3 $20.6Nmm\ deg^{-1}$
Torsional Spring 4	k_4 $28.4Nmm\ deg^{-1}$
Torsional Spring 5	k_5 $290Nmm\ deg^{-1}$

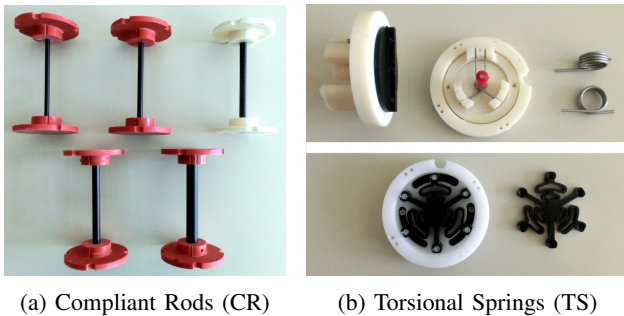


Fig. 3: Compliant elements used for the experiments: (a) Five compliant rods made in POM. (b) Top: torsional spring construction for TS1–4, using off-the-shelf springs; bottom: torsional spring for TS5, with a custom designed POM spring.

(used for TS1–TS4) was made using pairs of off-the-shelf torsional springs, slightly pre-compressed, mounted in a mirrored configuration so that they act one against each other (top row of Fig. 3b). This way, the resulting compliant element has the same stiffness value when rotated clockwise or counterclockwise. The range of motion of this design is ± 60 deg. The second TS design (used to get a higher stiffness value for TS5) was inspired by the work of Carpino et al. [13] (bottom row of Fig. 3b). This design was chosen because it is symmetrical along the direction of rotation, the stiffness value can be varied by changing the thickness, and it is quite compact and easy to manufacture. TS5 was made in POM

and has a range of motion of ± 30 deg.

Table II summarizes the different compliant elements that were used for the experiments. These values were chosen among a larger selection so that, during the locomotion of a RB meta-module, the most compliant elements (CR1 and TS1) could be naturally bent almost to their full range. Each of the next three elements (CR2–4 and TS2–4) roughly doubles the value of the previous one. The stiffest elements (CR5 and TS5) are of an order of magnitude higher than the previous, to provide an “almost stiff” test case. For the CR, the stiffness values were calculated using the cantilever beam theory (E: material’s Young’s modulus, I: moment of inertia, L: beam length; J: torsion constant; G: shear modulus):

$$\text{beam stiffness: } k_C = \frac{3EI}{L^3} \quad (1)$$

$$\text{torsional stiffness: } k_T = \frac{\pi JG}{180L}. \quad (2)$$

For the first TS design, it can be demonstrated that the total stiffness is equal to the sum of the two springs. Since we used off-the-shelf components, their stiffness value was provided by the manufacturer. For the second TS design, the stiffness value was estimated using finite elements analysis (FEA). It is worth pointing out that, for the experiments reported in this work, we were mostly interested in the order of magnitude and the relative stiffness value between different compliant elements, rather than their precise value.

C. Control Framework

The two Roombots modules were controlled using a network of six coupled non-linear oscillators representing a Central Pattern Generator (CPG) similar to the ones described in [5]. We designed an oscillator network topology which matched the hardware morphology, with one oscillator per degree of freedom (Fig. 4). The control inputs for this CPG are the amplitude A_i , the offset X_i , and the phase lags ψ_{ij} of each oscillator i . We use one common frequency for all oscillators ($\nu = 0.2$ Hz), bi-directional couplings follow the rule such that $\psi_{ij} = -\psi_{ji}$, all coupling weights are set to 0.5, and all oscillators have only nearest-neighbor coupling. For this work, we set the CPG output to produce oscillatory joint angle signals.

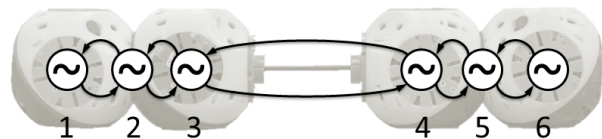


Fig. 4: CPG topology of a RB meta-module. Each of the six oscillators is assigned to one joint of the meta-module. All oscillators have nearest-neighbor coupling.

To reduce the number of open parameters, we used only one amplitude $A_i=A$, set the external oscillators (1 and 6) to a locked state, and set the offset for the oscillators 2 and 5 to zero (we assumed that the external geometry of the modules could be simplified with spheres). We did not however induce

TABLE III: Open CPG parameters used for the on-line PSO optimization. All values expressed in radians.

Variable	Range
Amplitude	[0.8 $\frac{3\pi}{4}$]
Offset X_3	[-1.2 1.2]
Offset X_4	[-1.2 1.2]
Phase lag $\psi_{23}=\psi_{32}$	$[-\pi \pi]$
Phase lag $\psi_{34}=\psi_{43}$	$[-\pi \pi]$
Phase lag $\psi_{45}=\psi_{54}$	$[-\pi \pi]$

any artificial symmetry, i.e. we did not apply any mirroring of parameter sets along our network, to avoid restricting the possible variety of parameters. Table III summarizes the open CPG parameters and their range of values.

In order to find the fastest gait for each type of compliant element, we let a population-based algorithm based on Particle Swarm Optimization (PSO) provide an automatic design of the CPG control input parameters. For this work, we discarded the possibility of running simulated (off-line) gait optimization experiments because of the difficulty to transfer them to the hardware robot. Compliant elements are in general complex to model and they often induce numerical instability which widens the gap between simulation and reality. Instead, all the parameters used herein were evolved using on-line optimization, with each particle of the PSO tested directly on the hardware modules. The typical optimization for one set of parameters consisted in 9 particles and 20 iterations (180 particles to be tested).

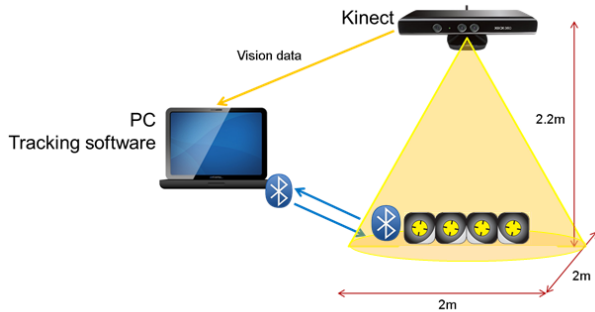


Fig. 5: Test arena used to run on-line parameter optimization.

The test arena used for on-line optimization was composed of a rubbery flat mat (used to alleviate the impacts of the robots with the ground) of approximate size of 2m by 2m, a Microsoft Kinect (mounted overhead) that tracks the position of the robots using its depth camera, and a control computer that runs the PSO algorithm (Fig. 5). For each trial, the computer generates the PSO particle containing the new CPG parameters to be tested. These are sent via Bluetooth to the Roombots meta-module which checks whether to accept the set of parameters using its internal collision detection. If the particle is discarded, a fitness value of zero is returned. Otherwise, the robot evaluates the parameters (using its on-board CPG controller) for 30 seconds. The first five seconds of the trials are not evaluated, in order to wait until the CPG

reaches a stable state. At the end of the trial, the computer measures the robot's displacement using the position data collected with the Kinect and calculates the fitness value: displacement divided by elapsed time. We did not restrict the evaluation of the speed to any specific direction, and, for this work, we did not minimize the sideways displacement. The position information provided by the Kinect is used solely for the fitness evaluation, while the CPG controller runs in open-loop.

D. Comparison methodology

Defining a good quantitative experimental protocol to evaluate and compare the effect of compliance in a robotic structure can be a quite challenging task since several factors are affected. In order to evaluate hypothesis 1 (improvement of performance), we compared the maximum speed that we were able to achieve for each configuration and stiffness value. In the data analysis, we also considered repeatability, a measure of the variability of the speed when repeating the same experiment multiple times. Since the CR configurations have a bigger size (5 RB grid units) compared to the TS (~ 4 RB grid units), we also considered the body-lengths per second as a simplistic method to compare different types of compliant elements.

Since the speed of locomotion depends both on the gait and on the type of compliant element used, and considering that a good gait for one element might not be well suited for another one, we developed the following experimental protocol to test hypothesis 3:

- We defined three test cases (*soft structure*, *medium structure*, and *stiff structure*) corresponding to the first, third, and fifth stiffness value for each type of compliant element.
- We ran a full on-line optimization of speed of locomotion for each of these three cases (a total of six optimizations) to find good sets of control parameters (*soft pattern*, *medium pattern*, *stiff pattern*), fit for the value of stiffness of each test case.
- We tested these patterns on structures with the same type of compliant element but different stiffness value and evaluated how well they performed.

III. EXPERIMENTAL RESULTS AND DISCUSSION

Following the methods described in the previous section, we ran six different on-line parameter optimizations, namely for CR1, CR3, CR5, TS1, TS3, and TS5, and obtained six sets of CPG parameters (*patterns*). We then tested each compliant element with all three sets of parameters obtained for that type of compliant element. We repeated each experiment 10 times (30 seconds per run) to test the repeatability of the gait. Using the Kinect tracking, we evaluated the displacement and thus the speed.

Figs. 6 and 7 show the mean speed value for each CR and TS experiment. The error bars represent the standard deviation of the 10 repetitions. The x-axes are represented in a logarithmic scale in order to properly fit the stiffness

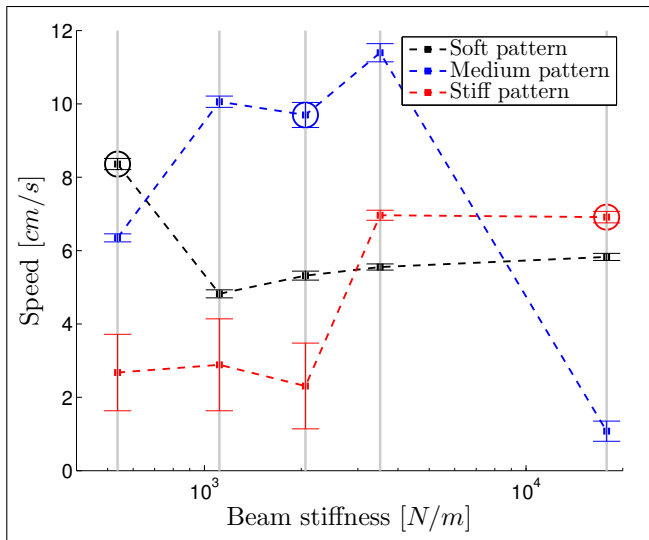


Fig. 6: Mean robot speed for each type of pattern with the Compliant Rod elements. The error bars represent the standard deviation for 10 repetitions. The circled data points are the direct result of on-line optimization.

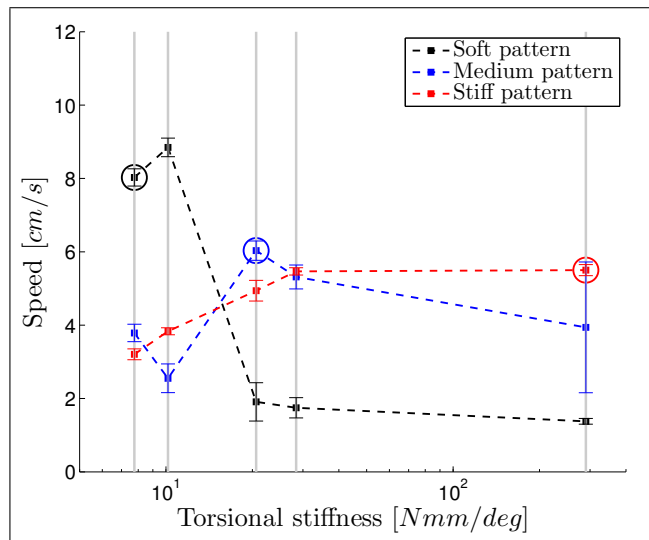


Fig. 7: Mean robot speed for each type of pattern with the Torsional Spring elements. The error bars represent the standard deviation for 10 repetitions. The circled data points are the direct result of on-line optimization.

values used herein. The circles represent the data points that have been optimized for that particular structure.

For the Compliant Rod (Fig. 6), the *medium pattern* can be used to achieve very good locomotion gaits while changing stiffness value (hypothesis 3), except for the *stiff structure*. For this configuration, the presence of compliance deeply affected the locomotion pattern. The *stiff pattern* produced a movement perpendicular to the main axis of the robot, with the modules generating some momentum in order to roll the

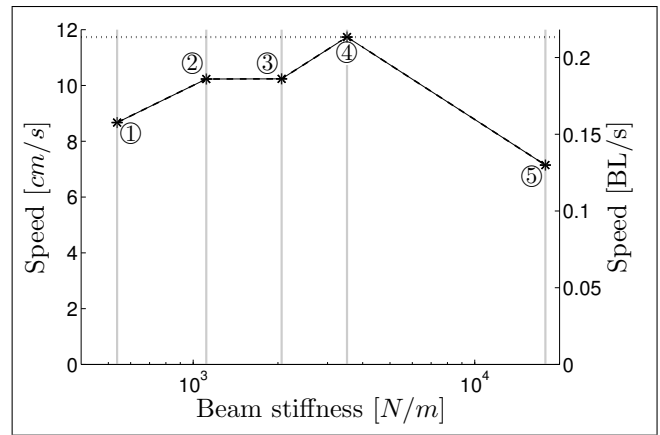


Fig. 8: Maximum robot speed with the Compliant Rod elements. The speed in body lengths per second was calculated using a length of five RB units (0.55m). Points two and four are not the result of a dedicated optimization but obtained by running the *medium pattern* CPG parameters.

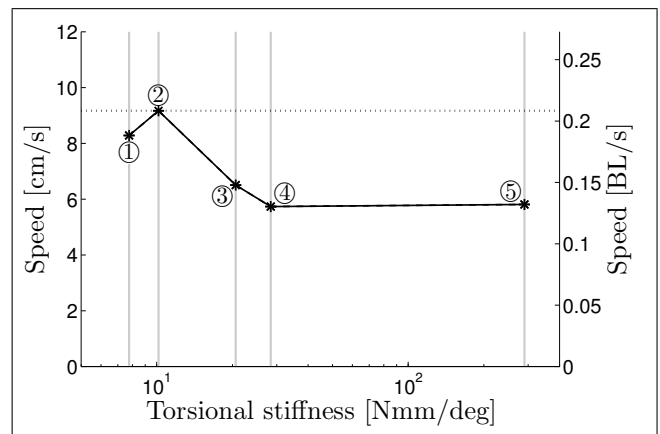


Fig. 9: Maximum robot speed with the Torsional Spring elements. The speed in body lengths per second was calculated using a length of four RB units (0.44m). Point two and four are not the result of a dedicated optimization. Point two was obtained by running the *soft pattern*; point four was obtained by running the *medium pattern* CPG parameters.

structure². This strategy failed when tested with compliant elements because it was not able to flip over. On the contrary, the *soft* and *medium patterns* generated a movement normal to the main axis, in which one module is always ahead and pulls the other module forward. The *medium pattern* performed badly with CR5 because after a few locomotion cycles the structured became unbalanced and flipped over.

For the Torsional Spring (Fig. 7), the *soft pattern* uses a crab-like motion that uses high amplitude and exploits the high deformability of the compliant element. It however fails at increased stiffness because the high amplitude makes the structure flip. The *stiff pattern* uses almost the same control

²Some of the most interesting locomotion gaits are shown in the video attached to this paper or available at the following link: <http://biorob2.epfl.ch/utls/movieplayer.php?id=267>

strategy, except for the amplitude that is much lower and keeps the structure stable. On the other hand, the *medium pattern* evolved using a completely different strategy that was not well suited for other stiffness values. Overall, the behavior of the Torsional Spring was quite different from that of the Compliant Rod (hypothesis 2).

Figs. 8 and 9 show the maximum robot speed that we achieved with the Compliant Rod and the Torsional Spring elements. The curves represented in the plots are the envelopes of the maximum values of Figs. 6 and 7.

For each type of compliant element, there seems to be an optimal level of compliance (hypothesis 1). For the Compliant Rod, we have a peak of performance for a medium level of compliance, with an increase of speed of almost 65% compared to the stiff case. For the Torsional Spring, instead, there is a peak for low stiffness values (57% more speed than the stiff case). This is because the modules are using the soft spring as an additional (almost with no resistance) degree of freedom.

IV. CONCLUSION

In this work we presented a preliminary study on compliance using structures made of Roombots. We ran dedicated on-line CPG parameter optimizations for six different configurations and evaluated the performance using the speed and the repeatability of the gait. Different types and values of compliance produced quite different gaits (hypothesis 2) and it was hard to predict how the gait would be affected by them. From the analysis of the results, we can say that there was a clear increase in performance after the introduction of in-series compliance (hypothesis 1), thus making compliance a possible way to partially tackle the hardware scalability challenge. Hypothesis 3 remains a partially open question, depending on the type of compliance that is added to the SRMR. For omnidirectional compliance, it is possible to transfer the optimized gait parameters with quite good results.

For future work, we would like to extend our study to different Roombots structures and to a larger number of compliant elements, including more in-series elements and also external compliant extensions. We also plan to consider other factors to better evaluate the effect of compliance on the locomotion of a SRMR, such as power consumption, impact forces, and measurement of the deformation of the compliant element.

Our final goal is to have passive compliant elements included in the self-reconfiguration framework, and have the Roombots choose which one to connect to in order to adapt its structural stiffness to new environmental conditions.

ACKNOWLEDGMENT

We thank Alexander Spröwitz, Soha Pouya, Yuriy Perov, Anh The Nguyen, and Frédéric Wilhelm for their support for testing, implementation, development, and characterization of RB modules. We thank Jesse van den Kieboom, who developed code for the PSO-based optimization framework. We gratefully acknowledge the technical support of André

Guignard, André Badertscher, Philippe Vosseler, Mitchell Heynick, Jean-Paul Brugger, Manuel Leitos, and Alfred Thomas.

REFERENCES

- [1] S. Murata and H. Kurokawa. Self-reconfigurable robots. *IEEE Robotics Automation Magazine*, vol. 14, no. 1, pp. 7178, March 2007.
- [2] J. Sastra. Using Modular Reconfigurable Robots for Rapid Development of Dynamic Locomotion Experiments. *Doctoral dissertation*, University of Pennsylvania, 2012.
- [3] M. Yim, K. Roufas, D. Duff, Y. Zhang, C. Eldershaw, and S. Homans. Modular Reconfigurable Robots in Space Applications. *Autonomous Robots*, vol. 14, no. 2-3, pp. 225-237, Mar. 2003.
- [4] M. Yim, S. Wei-Min, B. Salemi, D. Rus, M. Moll, H. Lipson, E. Billard, P. Dillenbourg, and A. J. Ijspeert. Modular Self-Reconfigurable Robot Systems [Grand Challenges of Robotics]. *IEEE Robotics & Automation Magazine*, vol. 14, no. 1, pages 43-52, 2007.
- [5] A. Spröwitz, S. Pouya, S. Bonardi, J. van den Kieboom, R. Möckel, A. Billard, P. Dillenbourg, and A. J. Ijspeert. Roombots: Reconfigurable Robots for Adaptive Furniture. *IEEE Computational Intelligence Magazine*, vol. 5, no. 3, pages 20-32, 2010.
- [6] M.H. Raibert. Trotting, pacing and bounding by a quadruped robot. *Journal of Biomechanics*, vol. 23, Supplement 1, pp. 79-98, 1990.
- [7] J.W. Hurst. The Role and Implementation of Compliance in Legged Locomotion. *Doctoral dissertation*, Carnegie Mellon University, 2008.
- [8] S. Aoi, H. Sasaki, and K. Tsuchiya. A Multilegged Modular Robot That Meanders: Investigation of Turning Maneuvers Using Its Inherent Dynamic Characteristics. *SIAM Journal on Applied Dynamical Systems*, vol. 6, no. 2, pp. 348-377, Jan. 2007.
- [9] C.H. Yu, K. Haller, D. Ingber, and R. Nagpal. Morpho: A self-deformable modular robot inspired by cellular structure. In *IEEE/RSJ International Conference on Intelligent Robots and Systems, 2008. IROS 2008*, pp. 3571-3578, 2008.
- [10] J. Sastra, W. G. Bernal-Heredia, J. Clark, and M. Yim. A biologically-inspired dynamic legged locomotion with a modular reconfigurable robot. In *Proc. of DSCC ASME Dynamic Systems and Control Conference*, Ann Arbor, Michigan, USA, 2008.
- [11] J. Sastra, S. Revzen, and M. Yim. Softer legs allow a modular hexapod to run faster. In *Climbing and Walking Robots (CLAWAR)*, 2012.
- [12] A. Spröwitz. Roombots: Design and Implementation of a Modular Robot for Reconfiguration and Locomotion. *Doctoral dissertation*, EPFL, Lausanne, 2010.
- [13] G. Carpino, D. Accoto, F. Sergi, N. Luigi Tagliamonte, and E. Guglielmelli. A Novel Compact Torsional Spring for Series Elastic Actuators for Assistive Wearable Robots. *Journal of Mechanical Design*, vol. 134, no. 12, pp. 121002-1–121002-10, Oct. 2012.